Optica Applicata, Vol. XVIII, No. 2, 1988

Measurement of refractive index profile in optical preforms using heterodyne interferometer of shearing type*

WACŁAW URBAŃCZYK, KAZIMIERZ PIETRASZKIEWICZ, WŁADYSŁAW WOŹNIAK

Institute of Physics, Technical University of Wrocław, Wybrzeże Wyspiańskiego 27, 50–370 Wrocław, Poland.

A non-destructive method of refractive index measurement in optical preforms is presented. Application of heterodyne interferometer of shearing type with rotating half-wave plate as a modulator results in considerable simplicity and high accuracy of measurements. With the method suggested the birefringence of the tested preform has no effect on measurement results. Algorithms of numerical reconstruction of refractive index profile, in which measurement data are approximated by power polynomials, are also presented. Usability of exemplary algorithms is estimated in the case of reconstruction of step-index and graded-index profiles.

1. Introduction

Measurements of refractive index profiles in optical preforms, based on non-destructive methods and applied so far, are carried out in the following way. The preform to be tested is immersed in the liquid of refractive index matching that of the preform cladding and illuminated by a plane wave propagating perpendicularly to its symmetry axis. The wave initially plane suffers from deformation when passed through the preform (Fig. 1**a**). If $W(x)$ represents the wave front shape in the space just behind the preform, then refractive index profile within the preform is calculated with the use of inverse Abel integral [1]

$$\Delta n(r) = n(r) - n_0 = -\frac{1}{\pi}\int_r^{r_0} \frac{\dfrac{dW(x)}{dx}}{\sqrt{r^2 - x^2}} dx \tag{1}$$

where: n_0 – refractive index of immersion, r_0 – radius of the preform.

At an early stage of optical fibre technology interferometric methods were most commonly used for refractive index profile measurements [2]–[5]. Interpretation of interference fringe patterns enables to the determination of wavefront shape $W(x)$ or its derivative $\dfrac{dW(x)}{dx}$ – depending on the type of the interferometer applied – and then calculation of the refractive index profile $\Delta n(r)$.

* This work was carried out under the Research Project CPBP 01.06.

However, in view of some shortcomings of classical fringe interferometry (such as troublesome automation of measurements, their low resolution and high cost of measuring instruments) new competitive solutions were being searched for. CHU [6] described the method of $\Delta n(r)$ determination by analysing the intensity of light reflected and refracted by the preform in the backward direction. WATKINS [7] proposed the preform scanning with extra narrowed laser beam. From the analysis of angular intensity distribution in the space behind the preform, the beam deflection angle $\varphi(x)$ can be determined (Fig. 1**b**). Taking into account relation $\frac{dW(x)}{dx} = \varphi(x)$,

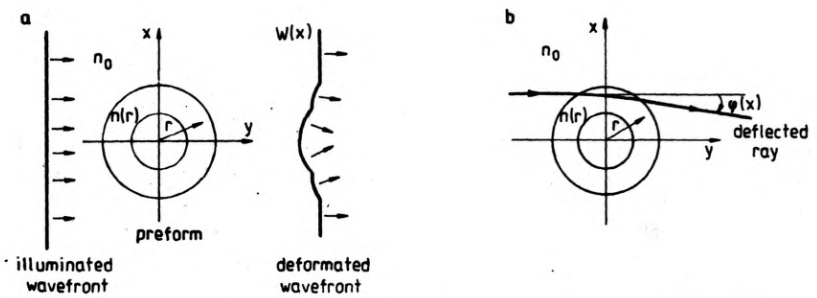

Fig. 1. Deformation of wavefront (**a**) and ray deflection (**b**) after passing through the preform tested

true for small deflection angles, one can easily calculate the refractive index distribution with the application of inverse Abel integral (1). MARCUSE [8] calculated the deflection angle $\varphi(x)$ from intensity distribution in defocused image of the preform. SASAKI et al. [9] arrived at $\varphi(x)$ using spatial filtering technique. However, it was the dynamic spatial filtering technique [10], in which the diaphragm rotating in the back focal plane of objective imaging the preform transforms the deflection angle into easily measurable time delay, that proved to be the simplest and the most accurate method of $\varphi(x)$ measurement. The technique of dynamic spatial filtering is applied to P101 and P102 Preform Analyser's made by York Technology.

The authors of the paper go back to the original idea of interferometric measurement. However, all the shortcomings of interferometric method are eliminated owing to the application of heterodyne technique. Practical applicability of a few algorithms of numerical reconstruction of refractive index profile has been checked. A computation method which is sufficiently fast and acceptably accurate has been chosen on the basis of the analysis. Accuracy of reconstruction has been estimated for typical step-index and graded-index profiles.

2. Measurement method

Let us assume that the preform to be tested is an isotropic object. Measurement method for the preforms of that type is illustrated in Fig. 2. Vertically positioned preform is illuminated by a plane wave, the azimuth of its polarization state being

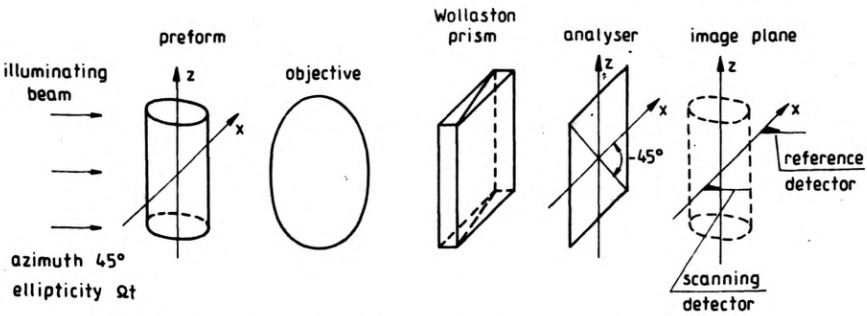

Fig. 2. Measurement method applied in the case of isotropic preforms

equal to 45° with regard to horizontal direction, and ellipticity modulated according to the formula $V(t) = \Omega t$, where Ω – frequency of modulation. This type of modulation introduces a linearly increasing with time phase shift between vertical and horizontal components of the light vector. There are two intensity detectors in the plane of the preform image: scanning detector and reference detector. Wollaston prism of horizontal bisection and analyser with transmission azimuth of $-45°$ with regard to the horizontal direction are placed in front of the image plane. Different values of refractive index within the preform induce the deformation of plane illuminating wave. Let $W(x)$ describe the shape of wavefront in the space just behind the preform (Fig. 3). Wollaston prism brings about splitting of the light wave passing through it so that two orthogonally polarized wavefronts (horizontal and vertical polarization) appear as a result in the image plane. This two wavefronts are identical

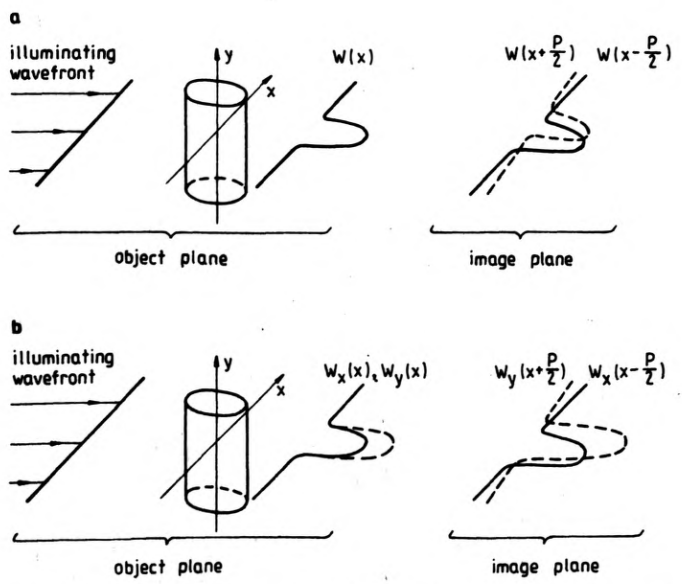

Fig. 3. Wavefront deformation after passing through isotropic (**a**) and anisotropic (**b**) preforms

in shape, however, they are shifted and inclined with regard to each other and total phase difference between them is given by the formula

$$\Phi(x) = k\left[W\left(x+\frac{p}{2}\right)-W\left(x-\frac{p}{2}\right)+\alpha x\right] \tag{2}$$

where: k – wavenumber, α – prism bisection angle, x – horizontal coordinate, p – shearing value. For small shearing – less than 5% of preform diameter – the above equation can be written in a simpler form

$$\Phi(x) = kp\frac{dW(x)}{dx}+\alpha x. \tag{3}$$

Analyser with transmission azimuth of $-45°$ with regard to horizontal direction, placed behind Wollaston prism, makes orthogonally polarized wavefront interfere. Vertical fringe pattern formed in the image plane is related only to the resultant phase difference

$$\Phi(x) = kp\frac{dW(x)}{dx}+\Omega t \tag{4}$$

where additional phase difference Ωt linearly increasing with time is introduced by ellipticity modulation of illuminating beam. The addend αx has been removed from formula (4) since it is related to the position of detectors only and does not change during the measurements. Fringe pattern formed in the image plane moves in horizontal direction with constant velocity due to the modulation. The signal from scanning detector is thus modulated sinusoidally

$$I_0(t) = 1+\cos\left[kp\frac{dW(x)}{dx}+\Omega t\right], \tag{5}$$

and its phase shift with regard to constant reference signal taken from the region outside the preform image

$$I_r(t) = 1+\cos(\Omega t) \tag{6}$$

is proportional to wavefront derivative $\frac{dW(x)}{dx}$. By moving the preform across the illuminating beam the wavefront derivative $\frac{dW(x)}{dx}$ can be measured point by point and then refractive index distribution $\Delta n(r)$ can be calculated according to formula (1).

Unfortunately, the idea outlined above cannot be directly applied to the measurements of anisotropic preforms. Usually considerable anisotropy occurs in most of the preforms due to residual internal stresses, resulting from the difference in thermal expansion coefficient of the cladding and that of the core. Owing to piezooptic effect the stressed preform becomes an anisotropic object of cylindrical symmetry, i.e., with principal axes perpendicular and parallel to its symmetry axis. As

a result it is already within the tested preform that the illuminating wave is split into two orthogonally polarized waves $W_x(x)$ and $W_y(x)$, see Fig. 3**b**. Let $W_m(x)$ denote the shape of mean wavefront in the region just behind the preform

$$W_m(x) = \frac{1}{2}[W_x(x) + W_y(x)], \tag{7}$$

and $R(x)$ – the difference of the polarized wavefronts

$$R(x) = W_y(x) - W_x(x).$$

It should be noticed that the function $W_m(x)$ is related only to the distribution of mean refractive index within the preform (averaging being carried out along principal axes), while $R(x)$ – only to its anisotropy. For anisotropic preforms the two split wavefronts generated in the image plane will no longer be identical

$$\begin{aligned} W_x(y) &= W_m\left(x - \frac{p}{2}\right) - R\left(x - \frac{p}{2}\right), \\ W_y(x) &= W_m\left(x + \frac{p}{2}\right) + R\left(x + \frac{p}{2}\right), \end{aligned} \tag{8}$$

which means that the measured phase shift will be

$$\Phi(x) = kp\frac{dW_m(x)}{dx} + kR(x). \tag{9}$$

Apart from the addend $kp\frac{dW_m(x)}{dx}$ which is of interest to us, also the function $kR(x)$ related to the anisotropy of the preform is included in Eq. (9). Unfortunately, for the majority of preforms the values of phase shift $kR(x)$ are fairly high and it is virtually impossible to eliminate the addend $kp\frac{dW_m(x)}{dx}$ from measurements results.

The above difficulties arising in the case of anisotropic preforms can be overcome by introducing a small modification to the measurement system shown in Fig. 2. It proves sufficient to set an ellipticity modulator between the tested preform and the Wollaston prism and to illuminate the preform by polarized wave with azimuth parallel or perpendicular to its symmetry axis. Now, only one wavefront $W_y(x)$ or $W_x(x)$ will appear in the space behind the preform and will then be modulated and split by Wollaston prism. The measured phase shift will now be equal to

$$\Phi(x) = kp\frac{dW_y(x)}{dx}, \tag{10}$$

and numerical computation will result in reconstruction of refractive index distribution. It is now worth noticing that the measurement of refractive index distribution in anisotropic preform is ambiguous. Illumination of such a preform perpendicularly to its symmetry axis results in refractive index distribution that

depends on polarization direction of illuminating beam. Measured phase shift will be equal to

$$\Phi(x) = kp\frac{dW_x(x)}{dx} \quad \text{or} \quad \Phi(x) = kp\frac{dW_y(x)}{dx}, \tag{11}$$

depending on the azimuth of polarization of illumination wave. Due to this fact difference in reconstructed refractive index profiles depending on the polarization azimuth can be observed. This kind of ambiguity occurs in all the non-destructive measurement methods and usually is not greater than 5×10^{-4}.

3. Measurement set-up and exemplary measurement results

A scheme of the measurement set-up is shown in Fig. 4. As the light source a 5 mW He-Ne laser is used. The preform to be tested is placed on the stage which can be shifted across the illuminating beam by a step motor with minimum step equal to

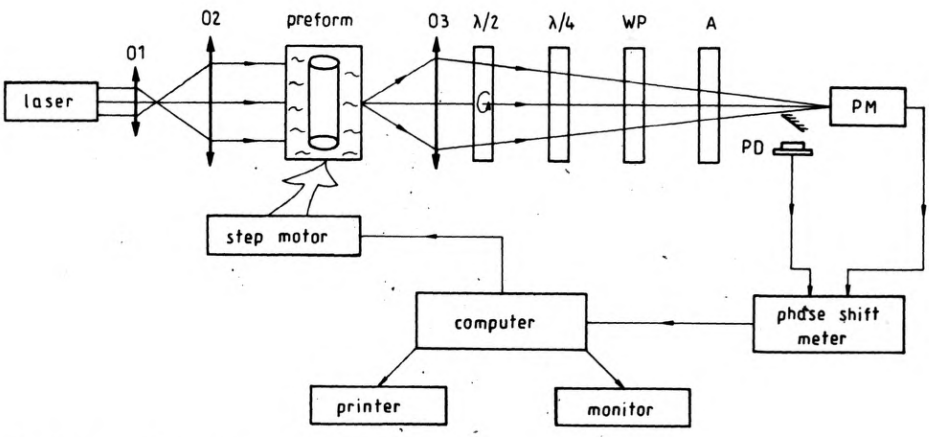

Fig. 4. Scheme of measurement set-up

5 μm. Ellipticity modulator consists of half-wave plate $\lambda/2$ rotating with 40 Hz frequency and stationary quarter wave plate $\lambda/4$ of azimuth 45° with regard to horizontal direction. Photomultiplier PM is used as scanning detector and photodiode PD placed in the region outside the preform image – as reference detector. Phase shift between signals from the photodiode and photomultiplier is measured by sampling with 4 MHz frequency. This results in theoretical measurement resolution better than $\lambda/10000$. Besides, it is possible to repeat the measurement several times and to average the results obtained for the same scanning point. Typically 16 measurements were averaged for one scanning point and that ensured measurement error to be of the order of $\lambda/1000$. Necessary computations were performed by measurement-controlling computer and refractive index distribution was obtained on TV monitor or on the printer as the need be. Time required

for the measurement and computation in the case of 250 scanning points was equal to about 7 min. Exemplary measurement results for single-mode and graded-index preforms are presented in Fig. 5.

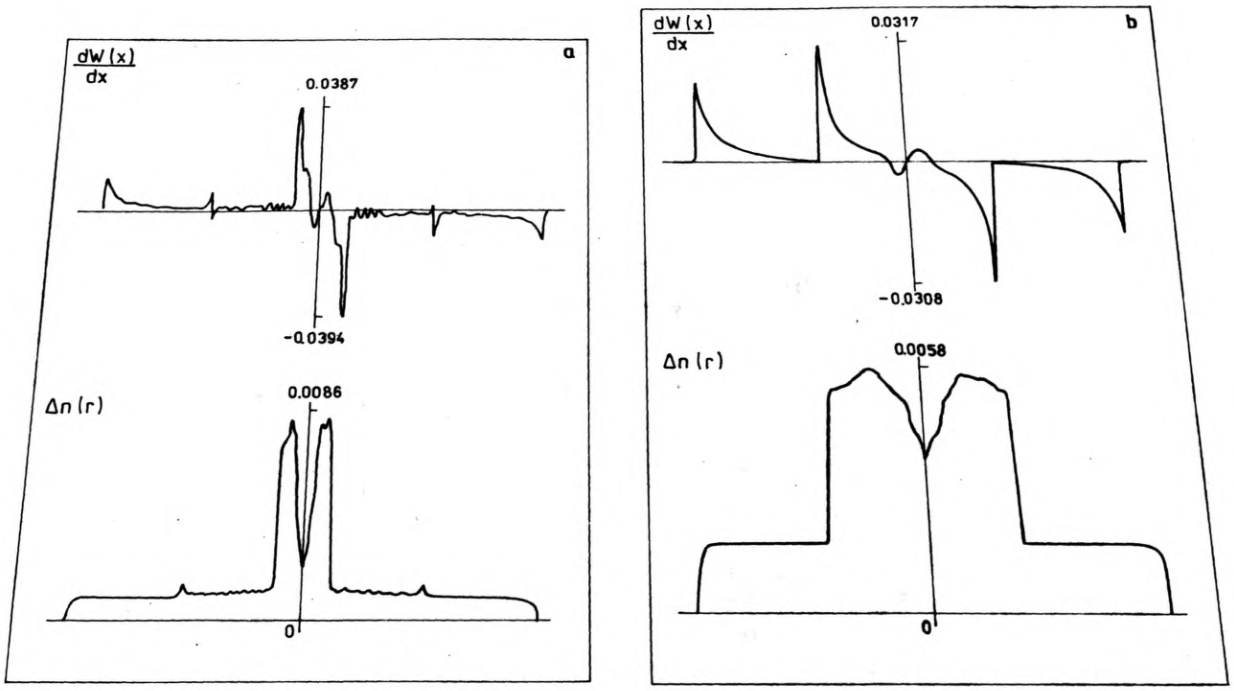

Fig. 5. Measurement results and reconstructed refractive index profile for single-mode (**a**) and step-index (**b**) preforms

4. Algorithm of refractive index reconstruction

Time of measurement is the basic problem in routine preform testing, most of the time being lost while calculating the refractive index distribution with the use of inverse Abel transform (1). Besides the computer speed, computation method is very important as well. A few possible algorithms of refractive index profile reconstruction were tested to enable the selection of optimum calculation method.

The integral (1) was calculated with the help of the idea suggested by BOCKASTEN in [11] and applied later also in [12]–[14], in which the integrand was locally approximated by polynomials. Optimum degree of polynomial approximation was determined for typical refractive index profiles applied in lightguide technology. The algorithms used were based on the fact that if the integrand can be presented in the form of p-degree polynomial

$$\frac{dW(x)}{dx} = \sum_{i=0}^{p} A_i x^i, \tag{12}$$

the inverse Abel integral can be expressed as

$$\int \frac{\sum_{i=0}^{p} A_i x^i}{\sqrt{x^2-r^2}} = \left(\sum_{i=0}^{p-1} B_i x^i\right)\sqrt{x^2-r^2} + B_p \ln\left|x+\sqrt{x^2-r^2}\right|. \tag{13}$$

Coefficients $B_0 \dots B_{p-1}$ and B_p are linear combination of $A_0 \dots A_p$. They can be determined by differentiating both sides Eq. (13) and then equating the expressions at coreresponding powers. Explicit form of the right-hand side of Eq. (13), for a few low-degree polynomials is presented in the Table.

Forms of approximating polynomial

Degree of approximating polynomial	For of approximating polynomial	Inverse Abel transform
0	A_0	$A_0\left\|\ln x+\sqrt{x^2-r^2}\right\|$
1	$A_1 x+A_0$	$A_1\sqrt{x^2-r^2}+A_0\left\|\ln x+\sqrt{x^2-r^2}\right\|$
2	$A_2x^2+A_1x+A_0$	$\left(\frac{A_2}{2}x+A_1\right)\sqrt{x^2-r^2}$ $+\left(A_0+\frac{A_2}{2}r^2\right)\ln\left\|x+\sqrt{x^2-r^2}\right\|$
3	$A_3x^3+A_2x^2+A_1x+A_0$	$\left(\frac{A_3}{2}x^2+\frac{A_2}{2}x+A_1+\frac{2A_3}{3}r^2\right)\sqrt{x^2-r^2}$ $+\left(A_0+\frac{A_2}{2}r^2\right)\ln\left\|x+\sqrt{x^2-r^2}\right\|$

It would be unreasonable to approximate all the measurement data $\frac{dW(x)}{dx}$ obtained for the whole diameter of the preform by a single polynomial; it would lead to inadmissibly long time of calculation in the case of polynomials of too high degree. Otherwise – in the case of low-degree polynomials – the information on actual behaviour of $\frac{dW(x)}{dx}$ would be lost. However, the measurement range can be divided into intervals and the integral (1) presented as the sum of integrals

$$\Delta n(r) = -\frac{1}{\pi}\sum_{k=1}^{N}\int_{x_k^d}^{x_k^g}\frac{\frac{dW(x)}{dx}}{\sqrt{x^2-r^2}}dx = -\frac{1}{\pi}\sum_{k=1}^{N}\widehat{I_k}(r). \tag{14}$$

where x_k^d and x_k^g – lower and upper integration limits in the k-th interval, respectively. Within the intervals the function $\frac{dW(x)}{dx}$ is substituted by polynomials of the type (12)

$$I_k(r) = \int_{x_k^d}^{x_k^g} \frac{\sum_{i=1}^{p} A_{i,k} x^i}{\sqrt{x^2 - r^2}} dx \tag{15}$$

where $A_{i,k}$ is the coefficient with x^i in k-th interval (Fig. 6). Finally, from (13), (14) and (15) we get

$$n(r) = -\frac{1}{\pi} \sum_{k=1}^{N} \left[\left(\sum_{i=0}^{p-1} B_{i,k} x^i \right) \sqrt{x^2 - r^2} B_{p,k} \ln \left| x + \sqrt{x + r^2} \right| \right]_{x = x_k^d}^{x = x_k^g}. \tag{16}$$

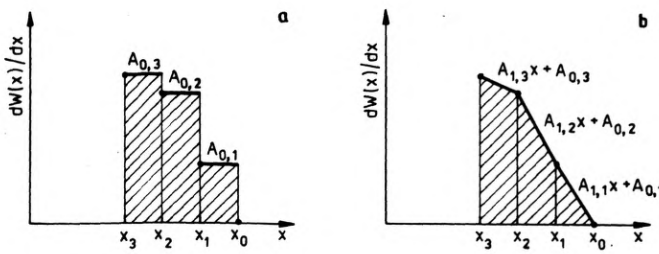

Fig. 6. Local approximation of the function $\frac{dW(x)}{dx}$ by zero degree (**a**) and first degree (**b**) polynomials. Points denote measurement data

To check the usability of formula (16) for reconstruction of refractive index distribution in preforms the computations were performed for two typical profiles $\Delta n(r)$. The values of derivative of Abel transform $\frac{dW(x)}{dx}$ were used as output data from measuring process. Two chosen functions and derivatives of their Abel transforms $\frac{dW(x)}{dx}$ are presented in Fig. 7. The functions represent refractive index profiles which are typical for optical preforms – step-index (Fig. 7**a**) and graded-index (Fig. 7**b**). Polynomials of the first, second and third degree and two values of N (number of measurement points) – 20 and 100 – were used in computation. Interpolation was applied in determining the coefficients A_i of polynomials. In the case of first polynomials, the points x_k and x_{k-1} were taken into account. For second degree polynomials the points x_k, x_{k-1}, x_{k-2}, and for third degree the points x_{k+1}, x_k, x_{k-1}, x_{k-1}, were considered.

In the case of step-index profile reconstruction, the number of measurement points (especially in the vicinity of $\Delta n(r)$ step edge) is more significant than the method of $\frac{dW(x)}{dx}$ approximation. This can be seen in Fig. 8, in which maximum error occurs always in the vicinity of $\Delta n(r)$ step edge. In the presented calculation the most unfavourable case of the measurement point not coincide with the step edge is assumed to occur, i.e., $\frac{dW(x)}{dx}$ is assumed to be equal to zero for $x = 1$, although actually $\frac{dW(x)}{dx} \to \infty$. It should be expected that in actual process of refraction index

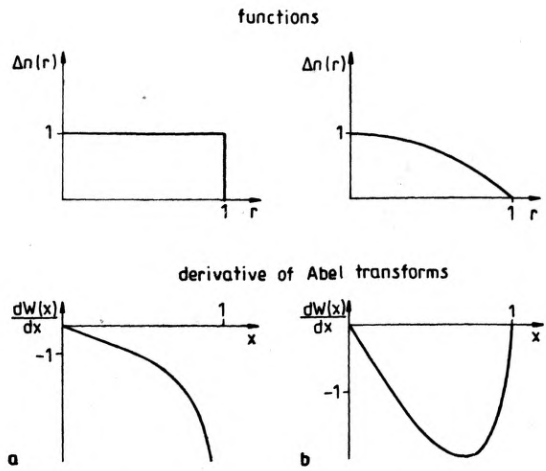

Fig. 7. Selected functions and derivatives of their Abel transforms: (a) function $\Delta(r) = \begin{cases} 1 & \text{for } r < 1 \\ 0 & \text{for } r \geqslant 1 \end{cases}$, derivatives of Abel transform $\frac{dW(x)}{dx} = \begin{cases} -2x(1-x^2)^{1/2} & \text{for } x < 1 \\ 0 & \text{for } x \geqslant 1 \end{cases}$, (b) function $\Delta n(r) = \begin{cases} 1-r^2 & \text{for } r < 1 \\ 0 & \text{for } r \geqslant 1 \end{cases}$, derivatives of Abel transform $\frac{dW(x)}{dx} = \begin{cases} -4x(1-x^2)^{3/2} & \text{for } x < 1 \\ 0 & \text{for } x \geqslant 1 \end{cases}$

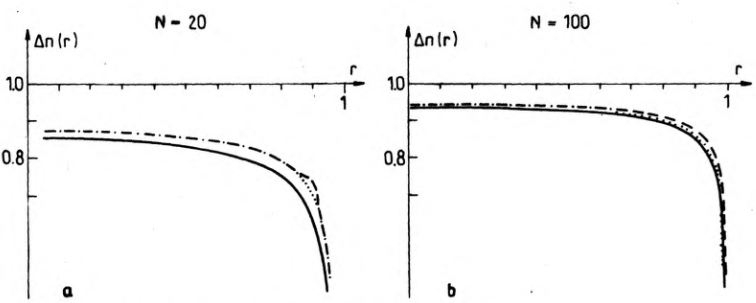

Fig. 8. Results of step-index profile reconstruction

profile reconstruction the error of $\Delta n(r)$ determination will be much smaller.

The error of graded-index profile reconstruction $\Delta n(r) = \Delta n_{\text{actual}}(r) - \Delta n_{\text{calc}}(r)$ is presented in Fig. 9. The application of higher order polynomials does not yield much higher accuracy of reconstruction. However, in the case of graded-index profiles the accuracy is better by the order of value than that for step-index profiles.

The following conclusions can be drawn from the numerical analysis:

i) The application of polynomial of the order higher than first to the approximation is of no avail.

ii) The accuracy of profile reconstruction is strongly affected by the number of scanning points, there should be no less than 200 of such points along perform diameter.

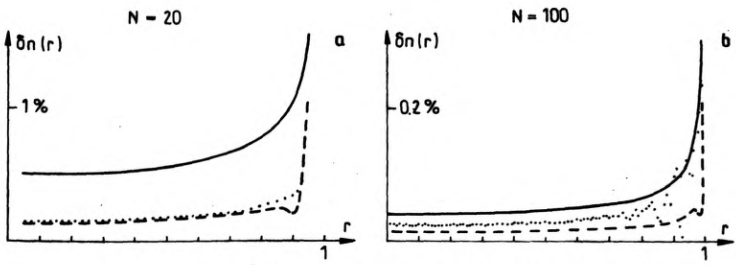

Fig. 9. Results of graded-index profile reconstruction. Reconstruction error $\delta n(r) = \Delta n(r)_{\text{actual}} - \Delta n(r)_{\text{calc}}$ is marked on vertical axis

iii) The error of smooth profile reconstruction is less than 0.2%, while for step-index profiles it is very large – up to 5%, and in the vicinity of step edge it may reach still higher values.

It should be stressed that in the analysis of reconstruction accuracy the formula (1) has been assumed to be always true. Actually, it is only an approximate relation since the rays refraction occurring within the preform is not taken into account. It can thus be supposed that the actual reconstruction error is larger than that resulting from the analysis performed, especially for preforms in which high gradients of refractive index occur. This error can be eliminated only by the application of reconstruction methods in which ray refraction within the preform is allowed for (see, e.g., [15], [16]).

5. Final remarks

The following features of the presented method of refractive index profile measurement in optical preforms are worth noticing:

i) direct measurement of wavefront deformation $\frac{dW(x)}{dx}$,

ii) high accuracy of measurement (rms = $\lambda/1000$),

iii) refractive index reconstruction accuracy higher than 0.2% for smooth profiles and higher than 5% for step-index profiles,

iv) low cost of measurement automation,

v) short time of measurement and treatment of results (a few minutes).

Accuracy and comfort of the measurement method suggested are thus comparable to the parameters achieved in – so far the best – dynamic spatial filtering method.

References

[1] VEST C. M., Appl. Opt. **14** (1975), 1601.
[2] OHTSUKA Y., SHIMIZU Y., Appl. Opt. **16** (1977), 1050.
[3] KOKUBUN Y., IGA K., Appl. Opt. **19** (1980), 846.

[4] KOKUBUN Y., IGA K., Trans. IECE of Japan **E60** (1977), 702.
[5] KOKUBUN Y., IGA K., Trans. IECE of Japan **E61** (1978), 184.
[6] CHU P. L., Electron. Lett. **13** (1977), 736.
[7] WATKINS L. S., Appl. Opt. **18** (1979), 2214.
[8] MARCUSE D., Appl. Opt. **18** (1979), 9.
[9] SASAKI I., PAYNE D. N., ADAMS M. J., Electron. Lett. **16** (1980), 219.
[10] SASAKI I., PAYNE D. N., MANSFIELD R. J., ADAMS M. J., [In] *Proc. Sixth European Conf. of Opt. Commun.*, York 1980, p. 140.
[11] BOCKASTEN K., J. Opt. Soc. Am. **51** (1961), 943.
[12] MARCUSE D., *Principles of Optical Fibre Measurement*, Academic Press, New York 1981.
[13] PAVELEK M., LISKA M., J. M. C., No. 2 (1985), 33.
[14] OHTSUKA Y., KOIKE Y., Appl. Opt. **19** (1980), 2866.
[15] SOCHACKI J., Appl. Opt. **25** (1986), 3473.
[16] GLANTSCHING W. J., J. Lightwave Techn. **LT3** (1985), 678.

Received October 1, 1987

Измерение профиля показателя преломления в световодовых заготовках при помощи гетеродинного интерферометра с поперечным сдвигом волнового фронта

Представлен интерференционный неразрушающий метод измерения распределения показателя преломления в световодовых заготовках. Простоты и большой точности измерения достигли, применяя гетеродинный интерферометр с поперечным сдвигом волнового фронта с вращающейся полволновой пластинкой в качестве модулятора. Предлагаемый метод способствует исключению влияния двойного лучепреломления исследуемой заготовки на результат измерения. Представлен также алгоритм численной реконструкции профиля показателя преломления при помощи локального приближения измерительных данных степенными многочленами. Сделана практическая оценка примерных алгоритмов в случае реконструкции ступенчатого и градиентного профилей.